Model investigation on the probability of QGP formation at different centralities in relativistic heavy ion collisions

Meiling Yu (喻梅凌),[1,2,*] Mingmei Xu (许明梅),[2,3] Zhengyou Liu (刘正猷),[1] and Lianshou Liu (刘连寿)[2,3,†]
[1]*College of Physics and Technology, Wuhan University, Wuhan 430072, People's Republic of China*
[2]*Key Laboratory of Quark & Lepton Physics, Huazhong Normal University, Ministry of Education, People's Republic of China*
[3]*Institute of Particle Physics, Huazhong Normal University, Wuhan 430079, People's Republic of China*
(Received 24 April 2009; published 14 December 2009)

The quantitative dependence of quark-gluon plasma (QGP)-formation probability ($P_{\rm QGP}$) on the centrality of Au-Au collisions is studied using a bond percolation model. The $P_{\rm QGP}$ versus the maximum distance $S_{\rm max}$ for a bond to form is calculated from the model for various nuclei and the $P_{\rm QGP}$ at different centralities of Au-Au collisions for the given $S_{\rm max}$ are obtained therefrom. The experimental data of the nuclear modification factor $R_{AA}(p_T)$ for the most central Au-Au collisions at $\sqrt{s_{NN}} = 200$ and 130 GeV are utilized to transform $S_{\rm max}$ to $\sqrt{s_{NN}}$. The $P_{\rm QGP}$ for different centralities of Au-Au collisions at these two energies are thus obtained, which is useful for correctly understanding the centrality dependence of the experimental data.

DOI: 10.1103/PhysRevC.80.064908 PACS number(s): 25.75.Nq, 12.38.Mh, 24.10.Lx, 64.60.ah

I. INTRODUCTION

It is believed that a medium with deconfined quarks and gluons as constituents, referred to as the quark-gluon plasma (QGP), can be created in high-energy nucleus-nucleus collisions. Up to now, a large amount of experimental data have been collected through the collisions of Si, O, Al, Cu, Au, Pb, and so on, at center-of-mass energies varying from about 2A to 200A GeV [1–8]. The recent data analyses of Relativistic Heavy Ion Collider (RHIC) Au-Au collisions at 200A GeV show strong evidence for liberated quark degrees of freedom over nuclear volumes [5–8].

The widely accepted definition for QGP is a (locally) thermally equilibrated state of matter in which quarks and gluons are deconfined from hadrons, so that color degrees of freedom become manifest over nuclear, rather than merely nucleonic, volumes [5]. From this definition, the formation of QGP requires quark deconfinement in a large volume, at least larger than that of a nucleon. Therefore, proton-proton collisions can certainly not form QGP, even at very high energy. For the same reason, it can be asserted that, the smaller the colliding nuclei, or equivalently, the more peripheral the collision of big nuclei, the less probability for QGP formation. This assertion has strong support from both experimental data and theoretical reasoning.

From the experimental side, the RHIC data on Au-Au collisions at various energies, $\sqrt{s_{NN}} = 200$, 130 GeV, and so on, found that, in the most central (0%–5% centrality) Au-Au collisions, the back-side high-p_T two-hadron correlations in the azimuthal angle disappear (i.e., the so-called monojet phenomenon [9]), which shows that, in central collisions, QGP is formed with high probability and absorbs the back-side jet. As centrality increases, the back-side jet appears gradually, indicating that the probability of QGP formation, denoted by $P_{\rm QGP}$, decreases continuously with the increase of centrality. While in the most peripheral collisions (60%–80% centrality) the back-side jets are observed in full strength just as in the case of p-p collisions.

The suppression of high-p_T hadron yields in a dense medium, quantified by the nuclear modification factor $R_{AA}(p_T)$, provides another experimental confirmation for the assertion. The factor $R_{AA}(p_T)$ is defined to be the A-A spectra relative to the p-p spectrum. It is believed that the suppression of hadrons at high p_T is of significance for final-state partonic energy loss in dense matter. Obviously, the greater the QGP-formation probability the more the suppression of hadrons. It is found that $R_{AA}(p_T)$ is most strongly suppressed for the most central collisions and becomes more and more weakly suppressed as centrality increases [10,11].

From the theoretical side, it is believed that QGP can be created if the energy density is above about ten times that of normal nuclear matter [12–14]. The energy deposition in the collision region is due to multiple scattering between nucleons from two incident nuclei. In the Glauber model [15], the probability of n multiscattering in the collision of two nuclei at a given impact parameter is a binomial distribution. For two head-on nuclei with identical nucleon number A, the mean number of multiscattering is proportional to $A^{4/3}$ [16]. Therefore, for small nuclei, the multiscattering number n may be large enough for QGP formation only at the tail of n distribution, which has negligibly small probability.

However, the previously mentioned arguments are only qualitative. A quantitative result on the probability of QGP formation versus the size of colliding nuclei or versus the centrality of the collision of big nuclei at different colliding energies is still lacking. Such a quantitative dependence of $P_{\rm QGP}$ on the size of the colliding nuclei, or on the centrality, is important in correctly understanding the data of various centralities at different energies. Let us take the nuclear modification factor $R_{AA}(p_T)$, which quantifies the suppression of a high-p_T particle in QGP, for example. This modification factor takes the p-p spectrum as a reference, that is, by definition $R_{p\text{-}p}(p_T) = 1$ at high p_T since there is no dense medium formed in p-p collision. Therefore the probability of QGP

*yuml@iopp.ccnu.edu.cn
†liuls@iopp.ccnu.edu.cn

formation $P_{\rm QGP}$ (where to simplify notation we will use in the following a single letter r for this probability) vanishes, $r = 0$. In contrast, the suppression in the most central A-A collisions will be the largest $R_{AA}(p_T|\text{most central}) = R_{AA\,\max}(p_T)$. For the collision with other centralities c, the values of $R_{AA}(p_T|c)$ will lie between $R_{AA\,\max}(p_T)$ and $R_{p\text{-}p}(p_T)$. We want to know quantitatively how much these values are. This can be achieved using the following simple formula. If the probability r of the QGP formation at different centralities, that is, if the functional dependence $r = r(c)$, is known, then

$$R_{AA}(p_T|c) = R_{AA\,\max}(p_T)\cdot r(c) + R_{p\text{-}p}(p_T)\cdot[1 - r(c)]. \tag{1}$$

The aim of the present article is to study the quantitative dependence of QGP-formation probability, r, on the size, A, of colliding nuclei, or on the centrality, c, of Au-Au collisions at various colliding energies.

Our study is carried out using a bond percolation model [17]. The application of percolation theory to quark deconfinement was first suggested by Baym [18] and further extended by Satz and co-workers [19–23]. In their work, they used a site percolation model and discussed the critical nucleon density of phase transition. In Ref. [17] the bond percolation model is applied to discuss the cluster formation in an analytic crossover between hadronic gas and QGP. We are now applying this model to study the probability of QGP formation.

First, let us have an intuitive look at the process that occurs in heavy ion collisions. When two nuclei collide with high velocity, Lorentz contraction causes the scale in the longitudinal direction to be much less than that in the transverse plane, and the two nuclei can be described as two disks without thickness. During the collision, the nucleons in the two disks interact with each other and the potential barriers between neighboring nucleons decrease with the increase of the colliding energy $\sqrt{s_{NN}}$. That is, the wave function of nucleons will be distorted at high energy, and the infinitely high confinement potential between neighboring nucleons might be reduced to a finite-height potential barrier [cf. the central subfigure in Fig. 1(a)]. The higher the colliding energy is the more distorted the nucleon wave function and the lower

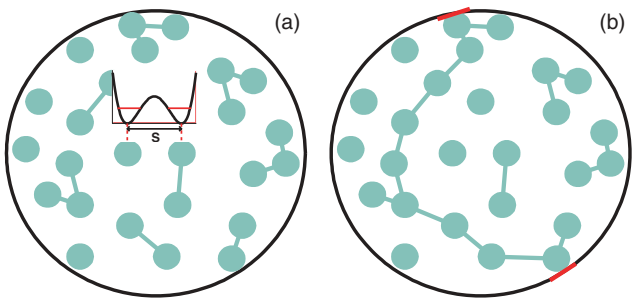

FIG. 1. (Color online) A schematic plot for the bond formation. (a) Nucleons connected by bonds form clusters. The central subfigure shows how the infinite confinement potential between two neighboring nuclei reduces to a finite-height potential barrier. Quark tunneling through the barrier forms bond, shown as full-line segments in the main figure. (b) A cluster extending from one boundary to another is an infinite cluster.

the potential barriers. As a result of quantum tunneling, the quarks in nucleons are able to delocalize from a single nucleon and the nearer the two nucleons the larger the probability of delocalization. Let us use S to denote the distance between the neighboring nucleons that have quark delocalization, [cf. the central subfigure of Fig. 1(a)]. At fixed energy $\sqrt{s_{NN}}$, there exists a maximum distance $S_{\max}$, such that quark delocalization is possible when $S \leqslant S_{\max}$ but is impossible when $S > S_{\max}$. The relation between $S_{\max}$ and $\sqrt{s_{NN}}$ is determined by the shape of the confinement potential. At relativistic high energies the contribution to this potential from the nucleon initial state, which at these energies are saturated gluons and current quark antiquark pairs, should be considered. In this article, as a first step, we focus on the percolation process and use experimental data as input to obtain the correspondence between $S_{\max}$ and $\sqrt{s_{NN}}$ (cf. the two vertical lines in Fig. 3). What we can infer at this step is that, as $\sqrt{s_{NN}}$ increases, the maximum delocalization distance $S_{\max}$ increases, that is, the dependence $S_{\max} = S_{\max}(\sqrt{s_{NN}})$ is a monotonically increasing function.

If quark delocalization happens between two nucleons the two nucleons are connected by a bond, shown as full-line segments in Fig. 1, to form a cluster, inside of which quarks are free to tunnel from one nucleon to the other and the nucleons are turned to colored objects referred to as *cells*. Only the whole cluster is a color singlet. The size of a cluster is defined as the number of cells included in it. It can be seen from Fig. 1(a) that the clusters can be of various sizes.

As the size of a cluster grows to the nuclear scale, that is, extending from one boundary to the other [cf. the big cluster in Fig. 1(b)], the color degree of freedom is manifested over the nuclear volume and QGP forms.

This picture can be realized by a two-dimensional bond percolation procedure. In the usual geometrical percolation model, the control parameter is the probability p of bond or site occupation [24]. When p equals a critical value p_c, an infinite cluster appears and the system turns from a disconnected phase to a connected phase. In our bond percolation model, the control parameter is the maximum delocalization distance $S_{\max}$, which depends on the collision energy $\sqrt{s_{NN}}$ of the two nuclei. If two nucleons depart with a distance less than $S_{\max}$, there can be a bond formed between them, representing the tunneling of quarks through the potential barrier. The nucleons (cells) aggregated through bonds form clusters. When $S_{\max}$ arrives at a critical value S_c, an infinite cluster appears and the medium changes from a color insulator to a color conductor, or from hadron phase to quark-gluon phase.

II. CONSTRUCTION OF A BOND PERCOLATION MODEL

In a percolation model, two head-on colliding nuclei with nucleon number A are simplified as two overlapped disks of radius $R = 1.2A^{1/3}$ and with $2A$ nucleons (cells) randomly distributed inside the region. In the site percolation models, the distribution of nucleons inside the big disk has no restriction. Two nucleons can be totally overlapped, lying one on the other. In our bond percolation model, to give enough room for the cells to move and for the bonds to be able to form between neighboring cells, the cells must have a "hard core" with radius

r_e, or equivalently a minimum distance $S_{\min}$ between the two neighboring cells, where $r_e = 0.5S_{\min} < r_c = 0.34$ fm. Here, r_c is the radius of 394 cells closely packed in a large disk of radius $R = 7$ fm (see the Appendix). In the calculation we take $r_e = 0.1$ fm. Two cells cannot be located nearer than $2r_e$. A cell that departs after cluster formation from the center of the big disk farther than $R - r_e$ is referred to as a *boundary cell*. Note that r_e is the radius of the "hard core" of cells moving in a nucleus with radius $R = 7$ fm. It is not the "hard core" of nucleons moving in free space.

Let us denote a cell with a center at $\boldsymbol{r}_\alpha$ as cell α. Only the cells with a center at $\boldsymbol{r}$ satisfying $S_{\min} \leqslant |\boldsymbol{r} - \boldsymbol{r}_\alpha| \leqslant S_{\max}$ can form bonds with the cell α. These are referred to as *bond-candidate* cells. In principle, the maximum number n_b of cells that can be connected with cell α by bonds are determined by the number n_p of partons inside cell α, which at relativistic high energy can be very large, in particular, larger than the number n_c of the bond-candidate cells of cell α. In that case, the largest number n_b of bonds connected to cell α will be equal to n_c instead of n_p.

The percolation procedure is as follows:

(i) Randomly select a cell α as a *mother cell*.

(ii) Find the *bond-candidate cells*. As just discussed, the largest number of bonds n_b that can be connected to cell α, in the case of $n_c < n_p$, is equal to the number of candidate cells n_c, which is not a very large number. In the calculation, the value of this number is unimportant since, according to the theory of percolation [25–28], the results of bond percolation are the same for different bond numbers provided $n_b \geqslant 3$. This was verified in Ref. [29] for $3 \leqslant n_b \leqslant 100$ using our model. So we randomly select three cells from the bond-candidate cells to form three bonds connected to the mother cell α. These are referred to as *daughters*. If the number of candidate cells is less than three, then the number of daughters is equal to the candidate number.

(iii) For every daughter of cell α find its bond-candidate cells from the remaining unbounded cells and randomly select two bond-candidate cells to form bonds. The cells connected to daughters are called granddaughters.

(iv) Repeat the procedure to granddaughters and granddaughters' daughters and so on, and we will get a cluster, which grows until no bond-candidate cell can be found.

(v) Then choose another cell β from the remaining unbounded cells as another mother cell, and repeat the procedure starting from Step (ii).

In this way, every cell is assigned to a cluster. In every cluster, find the boundary cells, if any, calculate the distance between every two boundary cells, and denote the maximum distance by d. A cluster with $d > \sqrt{2}R$ is called an *infinite cluster*. The probability P_∞ for the appearance of an infinite cluster is defined as

$$P_\infty = \frac{\mathcal{N}_\infty}{\mathcal{N}}, \tag{2}$$

where $\mathcal{N}_\infty$ is the number of events with an infinite cluster and $\mathcal{N}$ is the total number of events in the sample. In this model, P_∞ is taken as the probability $P_{\rm QGP}$ of the QGP formation and will, therefore, be denoted in the following by r.

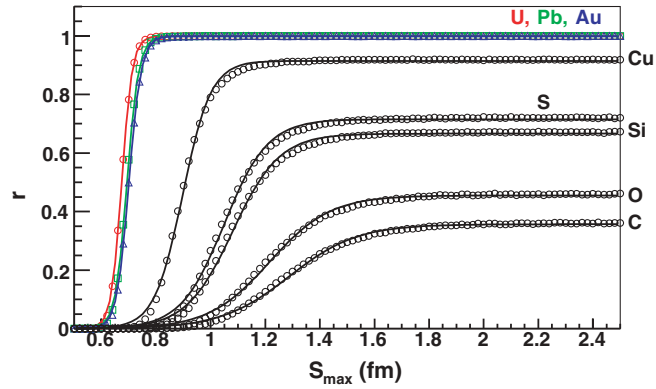

FIG. 2. (Color online) The probability r of an infinite cluster as a function of the maximum percolation distance $S_{\max}$ for nucleus-nucleus collisions of different nuclei calculated from bond percolation model. The statistical errors are within the symbols. The curves represent the fits to Eq. (3).

III. DEPENDENCE OF $P_{\rm QGP}$ ON SYSTEM SIZE AND CENTRALITY

The bond percolation simulation is done for nucleus-nucleus collisions of different nuclei. The variation of QGP-formation probability r as a function of $S_{\max}$ is shown in Fig. 2 for nuclei with the different nucleon number A. It can be seen that for each kind of nucleus, with the increase of $S_{\max}$, r gradually increases from 0 to a saturation value. This is typical for the finite-size percolation model, while for an infinite system $r(S_{\max})$ will be a step function and the point where r starts to be greater than 0 will be the threshold S_c. In our case, the system is of finite size, so we use a function [30]

$$r(S_{\max}) = a\{1 + \tanh\,[b(S_{\max} - f)]\}, \tag{3}$$

to fit the shape of $r(S_{\max})$ in Fig. 2, where a, b, and f are fitting parameters. It turns out that the fits are good (cf. the curves in Fig. 2). The inflection point f of the fitting curve can be used as an evaluation of the threshold of $S_{\max}$: $S_c = f$, and the saturation value of r is $r_{\rm sat} = 2a$. The results are listed in Table I.

TABLE I. The saturation value $r_{\rm sat}$ of $P_{\rm QGP}$ and the critical percolation distance S_c for different sizes of nuclei.

	U	Pb	Au	Sn	Cu	S	Si	O	C
A	238	207	197	119	64	32	28	16	12
$r_{\rm sat}$ (%)	100	99.8	99.8	98.7	91.4	71.6	66.6	45.4	35.6
S_c (fm)	0.67	0.69	0.70	0.78	0.90	1.05	1.08	1.22	1.29

From Table I, we see that larger nuclei have smaller S_c, which means that the energy threshold to form QGP for larger nuclei is lower than that of the smaller ones. The maximum QGP-formation probability $r_{\rm sat}$ for smaller nuclei are lower than those of the bigger ones. For small nuclei the QGP-formation probability is less than 100% even at very large $S_{\rm max}$, or, equivalently, at very high colliding energy $\sqrt{s_{NN}}$, that is the QGP-formation probability gets saturated. It can be seen from Table I that the saturation values $r_{\rm sat}$ of $P_{\rm QGP}$ for U-U, Pb-Pb, and Au-Au collisions are about 100%, while those of smaller nuclei do not reach 100%. For example, for Cu-Cu collisions only about 91% events form QGP at very large $S_{\rm max}$ (very high $\sqrt{s_{NN}}$). From the variation of $r_{\rm sat}$ on nuclear size A shown in Table I, we see that the saturation value $r_{\rm sat}$ of $P_{\rm QGP}$ decreases quickly when the nuclear size is less than that of copper.

Similar to Fig. 2, the relation between r and $S_{\rm max}$ for different centralities of Au-Au collisions can be calculated from the percolation model. The idea is that the probability to create QGP in noncentral collisions with the number of participants, $N_{\rm part}$, is equal to that in head-on collisions with nuclear size $A = N_{\rm part}/2$ at the same collision energy. Based on this idea, first we obtain the number of participants for different centralities of Au-Au collisions using the Glauber model, then $A = N_{\rm part}/2$ is taken as input to the bond percolation model to calculate the relation between r and $S_{\rm max}$. The resulting r versus $S_{\rm max}$ for different centralities of Au-Au collisions are shown in Fig. 3.

In the calculation, the $N_{\rm part}$ values are from the Glauber model for Au-Au collisions with beam energy 130A GeV [10]. We omit the slight dependence of $N_{\rm part}$ on beam energy. For example, for the most central collisions $\langle N_{\rm part}\rangle_{200\ \rm GeV}/\langle N_{\rm part}\rangle_{62.4\ \rm GeV} \approx 1.02$ [11,31], which makes a slight difference in the $r(S_{\rm max})$ distribution.

We can infer from Figs. 2 and 3 the dependence of QGP-formation probability r, on nuclear size A, or centrality c, for different $S_{\rm max}$. However, this is of little use because $S_{\rm max}$ is not a measurable quantity. The measurable quantity is the collision energy $\sqrt{s_{NN}}$. In applying the QGP-formation probability r calculated in our model to explain experimental data, we need to know the correspondence between $S_{\rm max}$ and $\sqrt{s_{NN}}$. In principle, the monotonically increasing function of $\sqrt{s_{NN}}$ versus $S_{\rm max}$ should be able to be calculated from a dynamical model, but there is not yet a reliable dynamical model. Therefore, we try to utilize the presently available experimental data to partly solve this problem.

The experimental results on the nuclear modification factor $R_{AA}(p_T)$ and the monojet (disappearance of back-side jet) show that both depart from the corresponding values of the p-p collision, the largest for the most central Au-Au collision at $\sqrt{s_{NN}} = 200$ GeV, but the departure is smaller from the corresponding p-p values for the same collisions at $\sqrt{s_{NN}} = 130$ GeV even for the most central collisions. This indicates that the formation probability r of QGP has (almost) arrived at saturation for the most central Au-Au collisions at $\sqrt{s_{NN}} = 200$ GeV but is unsaturated at $\sqrt{s_{NN}} = 130$ GeV. Based on this observation we assume that the central Au-Au collision at $\sqrt{s_{NN}} = 200$ GeV has *just arrived, or nearly arrived,* at *saturation*. From this assumption, we can get from Fig. 3 the $S_{\rm max}$ value of $\sqrt{s_{NN}} = 200$ GeV to be $S_{\rm max} = 0.90$ fm or a little smaller, where the QGP-formation probability r starts to saturate toward 100% for the most central Au-Au collisions.

Under this assumption, the QGP-formation probability $r(c)$ for different centralities c of $\sqrt{s_{NN}} = 200$ GeV Au-Au collisions can be obtained from the function $r(S_{\rm max})$ by taking $S_{\rm max} = 0.90$ fm [cf. the (red) dashed line in Fig. 3]. Once the function $r(c)$ is known, the model predicted $R_{AA}(p_T)$ for various centralities of 200A GeV Au-Au collisions can be calculated from Eq. (1), by taking the experimental $R_{AA}(p_T)$ data for 0%–5% centrality of Au-Au collisions at $\sqrt{s_{NN}} = 200$ GeV as the $R_{AA\,\rm max}(p_T)$ in this equation. The results are shown as (blue) solid curves in Fig. 4.

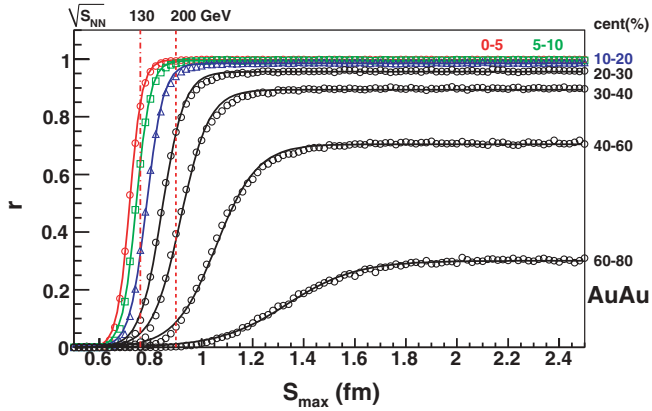

FIG. 3. (Color online) The probability r of an infinite cluster as a function of the maximum percolation distance $S_{\rm max}$ for Au-Au collisions at different centralities calculated from the bond percolation model.

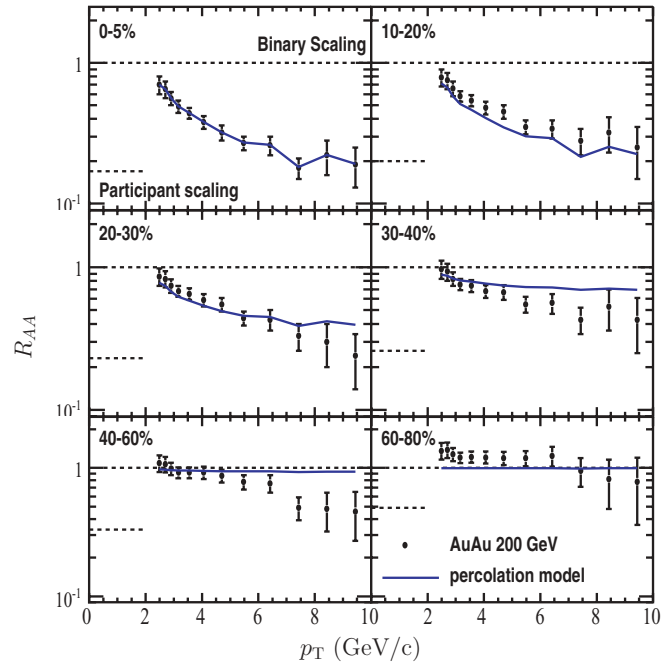

FIG. 4. (Color online) The comparison of $R_{AA}(p_T)$ between percolation model predictions and experimental data [11] for $\sqrt{s_{NN}} = 200$ GeV Au-Au collisions at various centralities.

When applying this method to other energies, for example, $\sqrt{s_{NN}} = 130\,\text{GeV}$ Au-Au collisions, we need to know the location of $\sqrt{s_{NN}} = 130\,\text{GeV}$ on the $S_{\max}$ axis of Fig. 3. For this reason, we make use of the experimentally observed $R^{\text{exp}}_{AA130}(p_T)$ for the most central ($c = 0\%$–5%) Au-Au collisions at this energy. The corresponding QGP-formation probability r value $r(c)|^{130\,\text{GeV}}_{c=0\%-5\%}$ can then be obtained through minimizing

$$\Delta = \sum_i \frac{\left[R^{\text{exp}}_{AA130}({p_T}^i|c = 0\%\text{–}5\%) - R^{\text{model}}_{AA130}({p_T}^i|c = 0\%\text{–}5\%)\right]^2}{\left[R^{\text{exp}}_{AA130}({p_T}^i|c = 0\%\text{–}5\%)\right]^2}, \tag{4}$$

where the superscript i indicates the different p_T bins, and the $R^{\text{model}}_{AA130}({p_T}^i|c = 0\%\text{–}5\%)$ are given by Eq. (1):

$$R^{\text{model}}_{AA130}({p_T}^i|c = 0\%\text{–}5\%) = R^{\text{exp}}_{AA200}({p_T}^i|c = 0\%\text{–}5\%) \cdot r(c)|^{130\,\text{GeV}}_{c=0\%-5\%} + R_{p\text{-}p}({p_T}^i) \cdot \left[1 - r(c)|^{130\,\text{GeV}}_{c=0\%-5\%}\right], \tag{5}$$

where the assumption that the QGP-formation probability r in the most central (0%–5%) Au-Au collision at 200A GeV has (just) reached saturation is used. In the minimizing process, $r(c)|^{130\,\text{GeV}}_{c=0\%-5\%}$ acts as the fitting parameter. The result is $r(c)|^{130\,\text{GeV}}_{c=0\%-5\%} = 84.32\%$. Then, from the functional dependence $r(S_{\max})$ shown in Fig. 3, it is easy to get the corresponding $S_{\max} = 0.76$ fm [cf. the (red) dash-dotted line in Fig. 3]. By knowing the location of $\sqrt{s_{NN}} = 130\,\text{GeV}$ on the $S_{\max}$ axis of this figure, the QGP formation probabilities r and the nuclear modification factor R_{AA} for different centralities of Au-Au collisions at this beam energy can be calculated using the same method as for 200A GeV Au-Au collisions. The resulting R_{AA} values for 130A GeV are shown in Fig. 5 as (blue) solid lines.

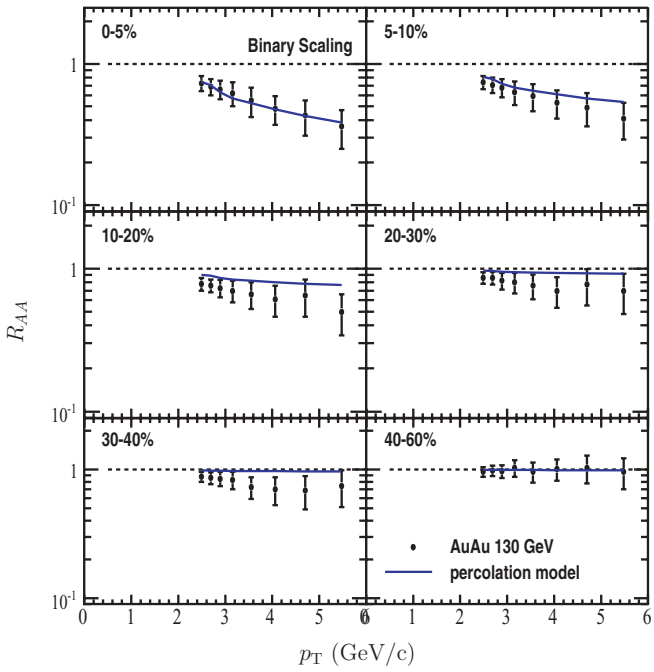

FIG. 5. (Color online) The comparison of $R_{AA}(p_T)$ between percolation model predictions and experimental data [10] for $\sqrt{s_{NN}} = 130\,\text{GeV}$ Au-Au collisions at various centralities.

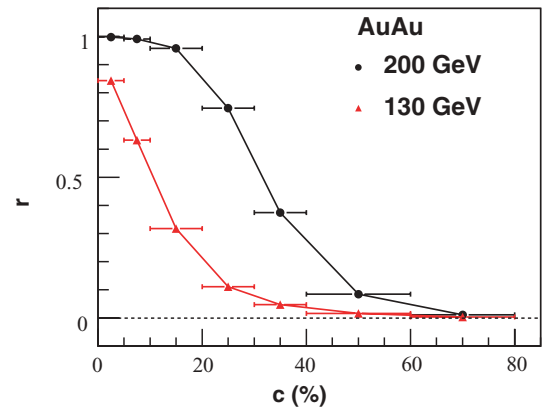

FIG. 6. (Color online) The QGP-formation probability r versus the centrality c of Au-Au collisions at $\sqrt{s_{NN}} = 200$ and 130 GeV.

We see from Figs. 4 and 5 that the model-predicted $R_{AA}(p_T)$ agree with the Au-Au experimental data at 200A and 130A GeV within error bars. These results support the application of our model to evaluate the probability of QGP formation at various centralities.

We can now obtain the dependence of QGP-formation probability r on the centrality c of Au-Au collisions for the two energies $\sqrt{s_{NN}} = 200$ and 130 GeV, as shown in Fig. 6. We see that both of them are a monotonically decreasing function. For Au-Au collisions at $\sqrt{s_{NN}} = 200\,\text{GeV}$, the probability r of the QGP formation drops to zero at 60%–80% centrality, whereas this probability for the same collisions at $\sqrt{s_{NN}} = 130\,\text{GeV}$ is vanishingly small already at 40%–60% centrality.

IV. CONCLUSION AND DISCUSSION

The probability of QGP formation at different centralities of Au-Au collisions is studied using a bond percolation model. A colliding-energy-dependent parameter $S_{\max}$ is introduced,

which is the maximum distance for a bond to form between two neighboring nucleons. The QGP-formation probability r versus $S_{\max}$ for different sizes of colliding nuclei, or for various centralities of Au-Au collisions, is calculated from the model, and the probability of QGP formation at different centralities of Au-Au collisions for given $S_{\max}$ are obtained accordingly. The experimental data of the nuclear modification factor $R_{AA}(p_T)$ for the most central Au-Au collisions at $\sqrt{s_{NN}} = 200$ and 130 GeV are utilized to transform the unmeasurable parameter $S_{\max}$ to the measurable colliding energy $\sqrt{s_{NN}}$. The probability of QGP formation at different centralities of Au-Au collisions for these two energies are then calculated from the model. The results are consistent with the experimental data within errors.

In the present paper, as a first step the correspondence between the model parameter $S_{\max}$ and colliding energies is simply derived by using experimental data. In the future, we plan to obtain the colliding energy dependence of $S_{\max}$ from theory. To do that, the confinement potential between quarks at zero temperature will be extended to high temperature by using QCD-inspired dynamical models in the framework of perturbative QCD at finite temperature.

ACKNOWLEDGMENTS

The authors thank Dr. Liu Hui for helpful discussions. This work was supported by NSFC under Project Nos. 10835005, 10775056, and 10847131.

APPENDIX: THE RADIUS OF SMALL CIRCLES CLOSELY PACKED IN A BIG CIRCLE

Consider the close packing of disks of radius r over some plane area in two dimensions, not allowing overlap (see Fig. 7). The plane can be partitioned into many hexagons. Disks cannot occupy the entire area. In a hexagon with area $6 \times \frac{2r\sqrt{3}r}{2}$ the area occupied by disks is $3\pi r^2$, resulting in an occupation rate of $\frac{\pi}{2\sqrt{3}}$. With this occupation rate, a big circle of radius $R = 7$ fm can accommodate 394 closely packed disks of radius $r = 0.34$ fm with the boundary effect neglected.

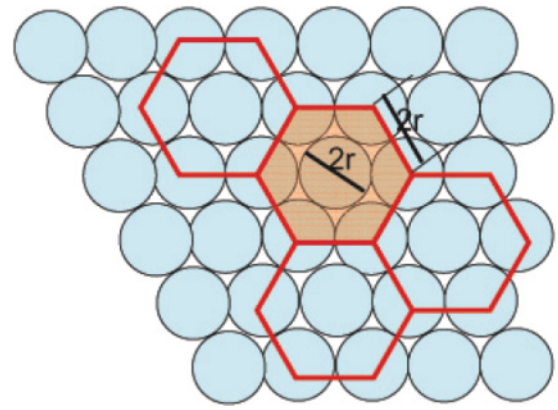

FIG. 7. (Color online) Close packing of small circles.

[1] T. Abbott *et al.* (E802 Collaboration), Phys. Lett. **B197**, 285 (1987).
[2] A. Bamberger *et al.* (NA35 Collaboration), Phys. Lett. **B184**, 271 (1987).
[3] R. Albrecht *et al.*, Phys. Lett. **B202**, 596 (1988).
[4] M. Jacob, CERN Preprint CERN-TH-5171-88 (1988).
[5] J. Adams *et al.* (STAR Collaboration), Nucl. Phys. **A757**, 102 (2005).
[6] K. Adcox *et al.* (PHENIX Collaboration), Nucl. Phys. **A757**, 184 (2005).
[7] B. B. Back *et al.* (PHOBOS Collaboration), Nucl. Phys. **A757**, 28 (2005).
[8] I. Arsene *et al.* (BRAHMS Collaboration), Nucl. Phys. **A757**, 1 (2005).
[9] M. Plümer, M. Gyulassy, and X. N. Wang, Nucl. Phys. **A590**, 511 (1995); C. Adler *et al.* (STAR Collaboration), Phys. Rev. Lett. **90**, 082302 (2003); J. Adams *et al.* (STAR Collaboration), *ibid.* **91**, 072304 (2003).
[10] C. Adler *et al.* (STAR Collaboration), Phys. Rev. Lett. **89**, 202301 (2002).
[11] J. Adams *et al.* (STAR Collaboration), Phys. Rev. Lett. **91**, 172302 (2003).
[12] J. D. Bjorken, Phys. Rev. D **27**, 140 (1983).
[13] F. R. Brown *et al.*, Phys. Rev. Lett. **65**, 2491 (1990).
[14] H. Satz, Int. J. Mod. Phys. A **21**, 672 (2006).
[15] R. J. Glauber, in *Lectures in Theorectical Physics*, edited by W. E. Brittin and L. G. Dunham (Interscience, New York, 1959), Vol. 1, p. 315.
[16] Cheuk-Yin Wong, *Introduction to High-Energy Heavy Ion Collisions* (World Scientific, Singapore, 1994), pp. 256–260.
[17] M. M. Xu, M. L. Yu, and L. S. Liu, Phys. Rev. Lett. **100**, 092301 (2008).
[18] G. Baym, Physica A **96**, 131 (1979).
[19] T. Celik, F. Karsch, and H. Satz, Phys. Lett. **B97**, 128 (1980).
[20] H. Satz, Nucl. Phys. **A642**, c130 (1998).
[21] H. Satz, Int. J. Mod. Phys. A **21**, 672 (2006).
[22] N. Armesto, M. A. Braun, E. G. Ferreiro, and C. Pajares, Phys. Rev. Lett. **77**, 3736 (1996).
[23] M. A. Braun and C. Pajares, Eur. Phys. J. C **16**, 349 (2000).
[24] K. Christensen and N. R. Moloney, *Complexity and Criticality* (Imperical College Press, London, 2005).
[25] J. Kertesz, B. K. Chakrabarti, and J. Duarte, J. Phys. A **15**, L13 (1982).
[26] D. S. Gaunt *et al.*, J. Phys. A **13**, 1791 (1980).
[27] S. G. Whittington, G. M. Torrie, and D. S. Gaunt, J. Phys. A **12**, L119 (1979).
[28] D. S. Gaunt, A. J. Guttmann, and S. G. Whittington, J. Phys. A **12**, 75 (1979).
[29] M. L. Yu *et al.*, Chin. Phys. C **33**, 552 (2009).
[30] H. W. Ke, M. M. Xu, and L. S. Liu, Chin. Phys. C **33**, 854 (2009).
[31] B. I. Abelev *et al.* (STAR Collaboration), Phys. Rev. C **79**, 034909 (2009).